AD-A172 211 250 MHZ/GHZ SCINTILLATION PARAMETERS IN THE EQUATORIAL POLAR AND AURORAL ENVIRONMENTS(U) EMMANUEL COLL BOSTON MA S BASU ET AL 28 MAR 86 AFGL-TR-86-0070 1/1

UNCLASSIFIED F19628-84-K-0003 F/G 4/1 NL

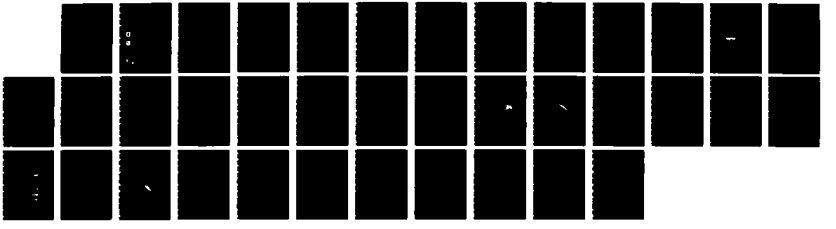

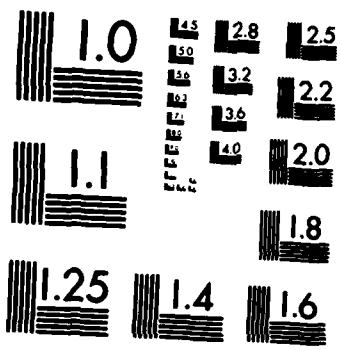

MICROCOPY RESOLUTION TEST CHART
NATIONAL BUREAU OF STANDARDS-1963-A

AD-A172 211

AFGL-TR-86-0070
ENVIRONMENTAL RESEARCH PAPERS, NO. 950

(12)

250 MHz/GHz Scintillation Parameters in the Equatorial, Polar and Auroral Environments

SANTIMAY BASU
E. MACKENZIE
SUNANDA BASU
E. COSTA
P.F. FOUGERE
H.C. CARLSON
H.E. WHITNEY

28 March 1986

Approved for public release; distribution unlimited.

DTIC
ELECTE
SEP 24 1986
S D
A

DTIC FILE COPY

IONOSPHERIC PHYSICS DIVISION

PROJECT 4643

AIR FORCE GEOPHYSICS LABORATORY

HANSCOM AFB, MA 01731

86 9 23 056

"This technical report has been reviewed and is approved for publication."

FOR THE COMMANDER

HERBERT C. CARLSON
Branch Chief

ROBERT A. SKRIVANEK
Division Director

This document has been reviewed by the ESD Public Affairs Office (PA) and is releasable to the National Technical Information Service (NTIS).

Qualified requestors may obtain additional copies from the Defense Technical Information Center. All others should apply to the National Technical Information Service.

If your address has changed, or if you wish to be removed from the mailing list, or if the addressee is no longer employed by your organization, please notify AFGL/DAA, Hanscom AFB, MA 01731. This will assist us in maintaining a current mailing list.

Unclassified
SECURITY CLASSIFICATION OF THIS PAGE

ADA172211

REPORT DOCUMENTATION PAGE

1a REPORT SECURITY CLASSIFICATION: Unclassified	1b RESTRICTIVE MARKINGS
2a SECURITY CLASSIFICATION AUTHORITY	3 DISTRIBUTION / AVAILABILITY OF REPORT: Approved for public release; distribution unlimited.
2b DECLASSIFICATION / DOWNGRADING SCHEDULE	
4 PERFORMING ORGANIZATION REPORT NUMBER(S): ERP, No. 950 AFGL-TR-86-0070	5 MONITORING ORGANIZATION REPORT NUMBER(S)
6a NAME OF PERFORMING ORGANIZATION: Air Force Geophysics Laboratory 6b OFFICE SYMBOL (If applicable): LIS	7a NAME OF MONITORING ORGANIZATION
6c ADDRESS (City, State, and ZIP Code): Hanscom AFB Massachusetts 01731	7b ADDRESS (City, State, and ZIP Code)
8a NAME OF FUNDING / SPONSORING ORGANIZATION 8b OFFICE SYMBOL (If applicable)	9 PROCUREMENT INSTRUMENT IDENTIFICATION NUMBER
8c ADDRESS (City, State, and ZIP Code)	10 SOURCE OF FUNDING NUMBERS

PROGRAM ELEMENT NO	PROJECT NO	TASK NO	WORK UNIT ACCESSION NO
62101F	4643	09	02

11 TITLE (Include Security Classification): 250 MHz/GHz Scintillation Parameters in the Equatorial, Polar and Auroral Environments

12 PERSONAL AUTHOR(S): Santimay Basu, E. MacKenzie,* Sunanda Basu,* E. Costa,* P.F. Fougere, H.C. Carlson, and H.E. Whitney

13a TYPE OF REPORT	13b TIME COVERED	14 DATE OF REPORT (Year, Month, Day)	15 PAGE COUNT
Scientific Interim	FROM ____ TO ____	1986 March 28	36

16 SUPPLEMENTARY NOTATION: *Emmanuel College Boston, MA 02115

This research was partially supported by Emmanuel College under Contract F19628-84-K-0003, and the Defense Nuclear Agency

17 COSATI CODES		
FIELD	GROUP	SUB-GROUP

18 SUBJECT TERMS (Continue on reverse if necessary and identify by block number)
Phase and intensity scintillation
Spectra — Phase spectral strength
Decorrelation time — Phase rate

19 ABSTRACT (Continue on reverse if necessary and identify by block number)

Ionospheric scintillation effects encountered in the equatorial anomaly crest, polar cap and auroral regions have been contrasted to provide information for the design and evaluation of the performance of satellite communication links in these regions. The equatorial anomaly region is identified as the most disturbed irregularity environment where the amplitude and phase structures of VHF/L-band scintillations are primarily dictated by the strength of scattering rather than ionospheric motion. In the anomaly region, the spectra of intense amplitude scintillations at VHF and L-band are characterized by uniform power spectral density from the lowest frequency (10 MHz) to 4 Hz at VHF and to 1 Hz at L-band and steep rolloff at higher fluctuation frequencies with power law indices of -5 to -7. Such structures are compatible with intensity decorrelation times of 0.1 and 0.3 sec at VHF and L-band frequencies, respectively. The phase spectra are described by power law variation of psd with frequency with typical spectral indices of -2.4. The strong scattering at VHF induces

(Contd)

20 DISTRIBUTION / AVAILABILITY OF ABSTRACT	21 ABSTRACT SECURITY CLASSIFICATION
☐ UNCLASSIFIED/UNLIMITED ☒ SAME AS RPT ☐ DTIC USERS	Unclassified

22a NAME OF RESPONSIBLE INDIVIDUAL	22b TELEPHONE (Include Area Code)	22c OFFICE SYMBOL
Santimay Basu	(617) 377-3141	AFGL/LIS

DD FORM 1473, 84 MAR — 83 APR edition may be used until exhausted. All other editions are obsolete.

SECURITY CLASSIFICATION OF THIS PAGE
Unclassified

19. (Contd)

extreme phase rates of 200° in 0.1 sec. The 90th percentile values of rms phase deviation at 250 MHz with 100-sec detrend are found to be 16 rads in the early evening hours whereas amplitude scintillation can cover the entire dynamic range of 30 dB not only at 250 MHz but at L-band as well. ~~In the polar~~ cap the 50th and 90th percentile values of rms phase deviation for 82-sec detrend are 3 and 12 rads respectively with comparable values being obtained in the auroral oval. The corresponding values for the S_4 index of scintillation are 0.5 and 0.8 in the polar cap which are slightly higher than those recorded in the auroral oval. The power law index of phase scintillation at high latitudes is in the vicinity of -2.3 which is not a result of very strong turbulence as in the equatorial region but is considered to be a consequence of shallow irregularity spectral indices. The phase rates at auroral locations are an order of magnitude smaller than in the equatorial region and attain values of 100° in 0.5 sec. The extreme variability of ionospheric motion in the auroral oval sensitively controls the structure of scintillations.

The long-term morphology (period 1979 to 1984) of intensity scintillations in the polar cap shows that in addition to the absence of diurnal variation of scintillations, and the presence of an annual variation with a pronounced minimum during local summer, there exists a marked solar control of scintillation activity such that it abruptly decreases when the solar activity falls below a threshold level.

Preface

These observations have been made possible by the cooperation of many individuals and organizations. M. D. Cousins of SRI International was responsible for the instrumentation and the initial software development was done by R. C. Livingston of SRI International. The efforts of F. Roberts of Logicon in modifying and adapting the software to the AFGL system are greatly appreciated. The authors would like to thank the Canadian Marconi Company and the Danish Arctic Contractors for their assistance in obtaining the Goose Bay and Thule data, respectively. This research was supported in part by AFGL Contract F19628-84-K-0003 and by the Defense Nuclear Agency.

Accession For
NTIS GRA&I ☑
DTIC TAB ☐
Unannounced ☐
Justification
By
Distribution/
Availability Codes
Dist | Avail and/or Special
A-1

Contents

Illustrations

250 MHz/GHz Scintillation Parameters in the Equatorial, Polar and Auroral Environments

1. INTRODUCTION

Satellite communication links in the VHF/UHF range can be subjected to the effects of ionospheric scintillations that are caused by the irregularities of electron density in the F-region of the ionosphere. These irregularities impose random phase perturbations on the wavefront of a satellite signal during its passage through the ionosphere. As the wavefront with perturbed phase travels towards the ground, intensity and phase fluctuations develop across the wavefront due to phase mixing. In the case of an orbiting satellite these intensity and phase fluctuations sweep past a receiver due to the satellite motion and the receiver output registers time variations of intensity and phase known as intensity or phase scintillations. On the other hand, in the case of a geostationary satellite, the motion of the ionospheric irregularities carries the intensity and phase variations across a fixed ray path and causes scintillations on a communications link. It should be remembered that the ray path from a satellite orbiting at an altitude of 1000 km sweeps past the ionospheric irregularities (assumed to be at 350 km) at a speed of ~ 3 km sec^{-1}. On the other hand, the speed of F-region irregularities relative to a receiver on the ground is typically on the order of 100 m sec^{-1}. As a result, the scintillation rate of orbiting satellite signals is generally an order of magnitude faster than those from geostationary satellites.

(Received for publication 28 March 1986)

Scintillations cause both enhancements and fadings about the median level of the signal as the radio signals sweep across the irregular ionosphere. When these fadings exceed the specified fade margin of a link, its performance is degraded. The degree of degradation will depend on the magnitude of fadings relative to the margin, the duration of the fade, the rate of fading, the type of modulation, and the criteria of acceptability. On a global scale, the degradations are most serious for propagation paths that transit the low latitude irregularity belt around the magnetic equator and the high latitude environment encompassing the auroral oval and polar cap regions (cf. Figure 1 given in Reference 1).

The morphology of scintillations has been studied for several years and documented for the equatorial, mid-latitude, auroral, and polar cap regions. Intensity scintillation measurements with orbiting and geostationary satellites provided the major data base for such long-term studies.[1] The morphology of phase scintillations was developed by the use of multi-frequency phase coherent DNA Wideband satellite transmissions in the equatorial[2] and auroral regions.[3,4] More recently, near-stationary polar beacon satellites that can be viewed at high elevation angles from high latitude stations have been used to develop the morphology of phase and intensity scintillations in the auroral oval and polar cap regions.[5] In addition, case studies of ionospheric scintillations have been made in conjunction with rocket, radar, satellite in-situ, and optical measurements.[6,7,8] These investigations have provided much insight into the mechanisms of irregularity formation and are expected to be helpful in developing predictive systems of scintillations based on geophysics.[9]

In this report, we first isolate very disturbed irregularity environments at both high and low latitudes, provide quantitative measures for the level of disturbance encountered by communication links in these regions, and analyze further the results in a form that can be used to evaluate communication system performance. We shall emphasize the difference between the structures of scintillation at high and low latitudes and isolate the appropriate parameters of concern to communication links operating in these two distinct disturbed regions of the globe.

2. DATA AND METHOD OF ANALYSIS

We have used both intensity and phase scintillation from Thule, Greenland (76.5° N, 68.7° W) a polar cap station; Goose Bay, Labrador (53.3° N, 60.3° W) located in the nighttime auroral oval; and Ascension Island (7.9° S, 14.4° W) an equatorial anomaly station where the critical frequency of the F2 layer attains high

---

(Due to the large number of references cited above, they will not be listed here. See References, page 27.)

values in the post-sunset period when the ionospheric irregularities become most pronounced.

At Ascension Island, 244-MHz signals from the geostationary satellite, Fleetsatcom, were recorded digitally by a computer controlled phase-lock receiver. The processing of the phase and intensity scintillation data using the phase-lock system has been described earlier.[10, 11] This system was operated over a limited period of time, namely January-February 1981 and January-February 1982, corresponding to periods of strong scintillation activity at this location. In addition to the above, total power receiving systems are employed to make routine recordings of signal intensity from Fleetsatcom at 244 MHz and from the geostationary satellite, Marisat, at a variety of frequencies, namely 257, 1541, and 3954 MHz. Round the clock observations by this total power system are recorded on chart recorders and manually analyzed to determine intensity scintillation magnitude over 15-min intervals.[12] During special campaign periods, however, the signals were recorded on magnetic tapes to perform spectral analysis and to evaluate both the first and second order parameters related to scintillation statistics.

At the high latitude stations, Thule and Goose Bay, 250 MHz signals from near-stationary polar beacon satellites were received at high elevation angles by both the computer controlled phase locked receiver and the total power system. In view of the periodic frequency updating of this satellite at 168-sec intervals, the phase and intensity scintillation data could be processed over 82-sec intervals spaced 168 sec apart.[5] The total power system acquired intensity scintillation data on chart recorders on a round-the-clock mode which were analyzed manually as mentioned earlier.

3. RESULTS

3.1 Ascension Island

During the last sunspot maximum period, the most severe scintillation activity was encountered at this equatorial station.[13, 14] Figure 1 shows a sample of such an extreme case of scintillation activity which was recorded on multi-frequency transmissions from Marisat. The left-hand panel shows from the top, intensity scintillations at 3954, 1541, and 257 MHz over a 3-min period in the early evening hours. The right-hand panel shows the corresponding power spectra for the samples. On the left-hand panel, the second central moment of signal intensity, namely the S_4 index of intensity scintillations defined in Reference 15 is labelled to provide a

---

(Due to the large number of references cited above, they will not be listed here. See References, page 27.)

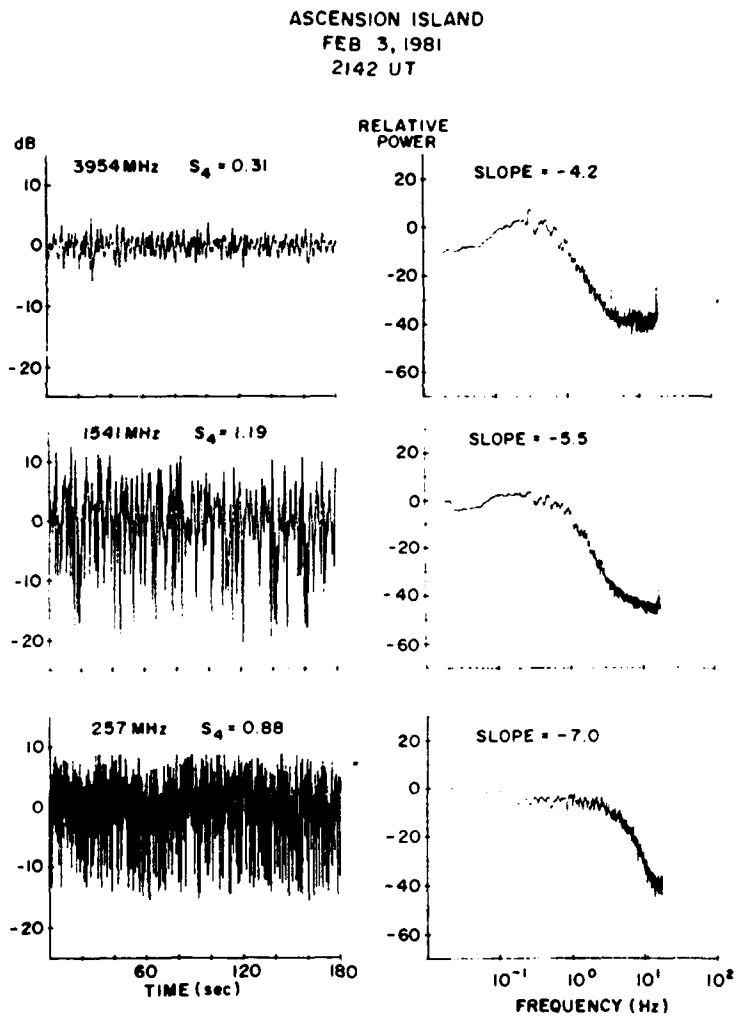

Figure 1. Three-min Data Segments of Scintillations at 3954, 1541, and 257 MHz Obtained at Ascension Island and Their Spectra. The S_4 index of scintillations and the power law index (slope) of the best fit straight line to the linear roll-off portions are indicated on the diagram

quantitative measure of intensity fluctuations. At the lowest frequency, 257 MHz shown in the bottom panel, the S_4 index of scintillations attains a value of 0.88 approaching the saturation condition of $S_4 \sim 1$. The rate of fading is extremely fast and approaches the receiver time of 0.1 sec. A receiver with larger dynamic range and faster response time would have recorded fading depths much larger than the 15-dB level registered in the figure. At higher frequencies the

phase perturbations are reduced so that scintillation magnitudes are expected to be less. In general, when scintillations are not very intense ($S_4 < 0.6$), intensity scintillation magnitudes (S_4) follow a frequency (f) dependence of $f^{-1.5}$ shown in Reference 16. The middle panel, however, shows that at 1541 MHz in the L-band, the S_4 index remains at the saturated level somewhat exceeding unity. This signifies that the irregularity environment is so intense that saturated scintillations are obtained at L-band (1541 MHz) and the VHF (257 MHz) scintillations are driven far into saturation. The level of activity can be gauged from the top panel which shows that even in the C-band (3954 MHz) scintillation with $S_4 = 0.31$ is obtained. From an engineering standpoint, this corresponds to a fluctuation of 6 dB.[17]

The power spectra of scintillations obtained by the use of fast Fourier transform (FFT) algorithm are shown in the right-hand panel as already mentioned. These provide much information on the temporal structure of scintillations and show the variation of power spectral density (psd) in decibels with the logarithms of fluctuation frequency.[18] The discussion of the spectra is facilitated if we start from the top panel which corresponds to weak scintillations at 3954 MHz. The scintillation spectrum at 3954 MHz is characterized by maximum psd at a frequency (f_m) of about 0.4 MHz. This frequency can be expressed as $f_m = u/\sqrt{2\lambda z}$ where u is the drift speed of irregularities orthogonal to the propagation path, λ is the radio wavelength and z is the slant range from the observing site to the irregularities.[19] Assuming a typical height of the equatorial F layer in the early evening hours as 400 km, the slant range can be derived as z = 450 km from the geometry of the observations. Substituting the values of $\lambda = 0.076$ m, z = 450 km, and $f_m = 0.4$ Hz in the above expression, the value of u is derived as 104 m sec^{-1}. In the equatorial region, during the early evening hours the drift speed of F-layer irregularities with respect to the ground generally vary between 100 to 200 m sec^{-1} as shown in Reference 20. Thus, the derived drift speed is in reasonable agreement

16. Rufenach, C. L. (1974) Wavelength dependence of radio scintillation: Ionosphere and interplanetary irregularities, J. Geophys. Res., 79:1562-1566.

17. Whitney, H. E. (1974) Notes on the Relationship of Scintillation Index to Probability Distributions and Their Uses for System Design, Rpt. AFCRL-TR-74-0004, AD 778092, Air Force Cambridge Research Laboratory, Hanscom AFB, Massachusetts.

18. Basu, Su., Basu, S., McClure, J. P., Hanson, W. B., and Whitney, H. E. (1983) High-resolution topside in-situ data of electron densities and VHF/GHz scintillations in the equatorial region, J. Geophys. Res., 88:403.

19. Franke, S. J., and Liu, C. H. (1983) Observations and modeling of multifrequency VHF and GHz scintillations in the equatorial region, J. Geophys. Res., 88:7075.

20. Basu, S., and Whitney, H. E. (1983) The temporal structure of intensity scintillations near the magnetic equator, Radio Sci., 18:263.

with the observed values. On the other hand, in view of the factor of two variation of drift, f_m can be estimated with relatively small uncertainty when the radio wavelength and the geometry of observations is known. In contrast to the above, the drift speed in the auroral oval can vary by a factor of ten or more, which can shift f_m considerably for a given geometry and a specified frequency as will be shown later in this report. The other features to be noted are the slopes of the spectra on either side of the maximum psd. Since both psd and frequency are plotted on a logarithmic scale, a linear slope indicates a power law variation of psd with frequency. The spectrum indicates that at the low frequency end, the variation can be approximated by f^{+1} and the variation of psd at the high frequency end can be expressed by $f^{-4.2}$. These spectral slopes are typically observed and have been related to the spectra of ionospheric irregularities[18] based on which the scintillation spectra have been successfully modelled theoretically.[19]

The middle right-hand panel shows the spectrum of 1541-MHz signals that represents the case of saturated scintillations. In contrast to the 3954-MHz spectrum discussed above, the spectral maximum in this case is broad and covers a frequency range of 0.1 Hz to 1 Hz. The high frequency slope is also steeper indicating a power law index of -5.5. The broad spectral width and steep spectral slopes are characteristics of strong intensity scintillations.[21, 22, 19] In fact, on the basis of the expression for f_m given in the previous paragraph which is valid for weak scintillations, one expects that at 1541 MHz a lower value of f_m will be obtained. Instead, f_m extends to much higher values due to strong scattering.[23] Since the auto-correlation function and power spectra are Fourier transform pairs, the increased spectral width signifies a shorter autocorrelation interval. Henceforth, the time interval for 50 percent decorrelation will be referred to as the decorrelation time (τ). For practical purposes, it is found that the inverse of the frequency f = 2 Hz, namely 0.5 sec, where the psd falls to a level of 20 dB below the maximum, corresponds quite well to the decorrelation time.

The lowest panel shows the scintillation spectrum of 257-MHz transmissions which is driven far into saturation. The spectral broadening is extreme in this case and extends to 4 Hz. The spectral slope is steepest and corresponds to a power law index of -7. The decorrelation time is found to be 0.13 sec signifying an extreme fading rate. It should be noted that although the S_4 indices for both 1541 and 257 MHz are approximately unity indicating saturation, the decorrelation interval

21. Rino, C. L. (1980) Numerical computations for a one-dimensional power law phase screen, Radio Sci., 14:41.

22. Booker, H. G., and MajidiAhi, G. (1981) Theory of refractive scattering in scintillation phenomena, J. Atmos. Terr. Phys., 43:1199.

23. Rino, C. L., and Owen, J. (1980) The time structure of transionospheric radio wave scintillation, Radio Sci., 15:479.

still varies becoming shorter at the lower frequency which suffers stronger scattering.

Figures 2a, 2b, and 2c show the cumulative distribution function (cdf) of signal amplitude for the three frequencies illustrated in Figure 1. The cdf is a first order statistic and is useful for defining the minimum margin requirements for communication links in non-diversity systems. The diagrams indicate the cdf for the observations (solid line) as well as the theoretical Nakagami m-distribution discussed in Reference 24 which is indicated by dotted lines at the m value ($m = 1/S_4^2$) appropriate for the data sample. It can be seen that the theoretical distributions represent the observations quite well over a wide range of activity levels, being weak at 3954 MHz and strong at both 1541 and 257 MHz. For intense scintillations the cdf approaches a Rayleigh distribution (m = 1). The Nakagami m-distribution has been earlier shown to be useful for describing the effects of scintillations on satellite communication links.[25]

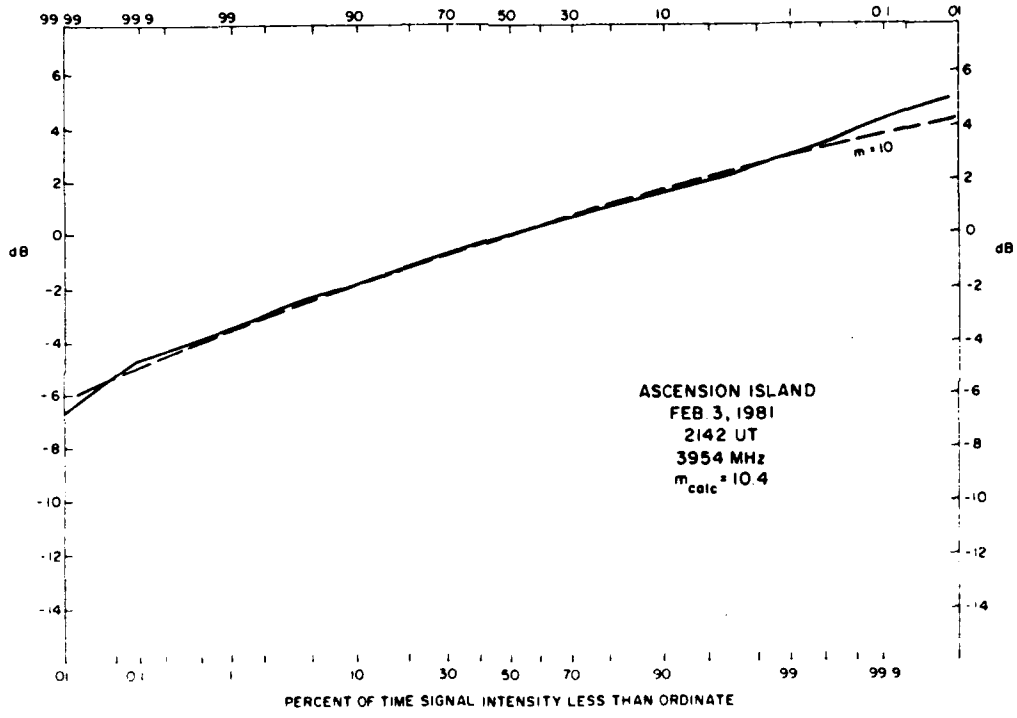

Figure 2a. The Cumulative Amplitude Distributions of Scintillations at 3954 MHz Shown in Figure 1. The theoretical Nakagami m-distribution for m = 10 is illustrated by dotted lines

24. Nakagami, M. (1980) The m-distribution—a general formula of intensity distribution of rapid fading, Statistical Methods of Radio Wave Propagation, W.C. Hoffman, Ed., Symposium Publications Div., Pergamon Press, New York.

25. Whitney, H.E., Aarons, J., Allen, R.S., and Seeman, D.R. (1972) Estimation of the cumulative amplitude probability distribution function of ionospheric scintillations, Radio Sci., 7:1095-1104.

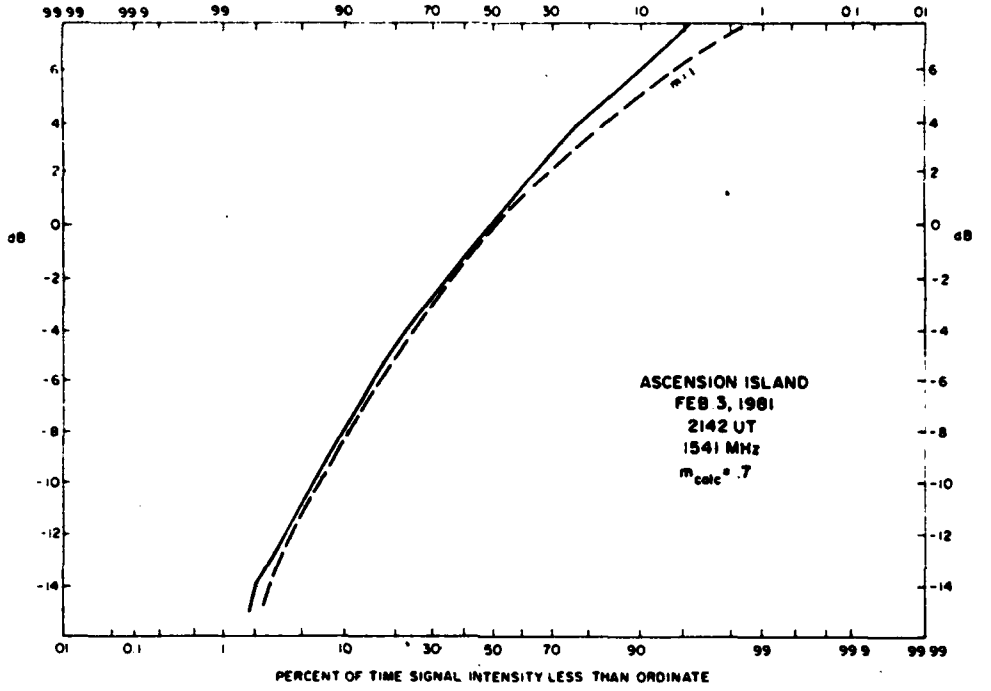

Figure 2b. The Cumulative Amplitude Distributions of Scintillations at 1541 MHz Shown in Figure 1. The theoretical curve in dotted lines illustrates the Nakagami-m distribution for m = 1 or Rayleigh distribution

In addition to cdf, which describes the probability distribution of the depth of fading, a statistical description of the fading rate is necessary to fully characterize the effects of scintillations on communication links. The information on the fading rate is contained in the power spectra of scintillations that we have described earlier. Another way of obtaining this information is to employ a level crossing technique. This gives the distribution of fade duration across a set of specified fading levels. Often, this representation is simpler and easier to interpret in relation to systems applications. The left- and right-hand panels in Figure 3 show the distribution of fades obtained at 3954 and 1541 MHz, respectively, over the first 1.5 min of the 3-min signal segments illustrated in Figure 1. The shortest fade duration that could be measured in conformity with the data digitization rate was 0.04 sec. The left-hand panel shows the distribution of fade duration for the 3954-MHz scintillation sample. Four separate fade depth levels at 1 dB intervals are found to be appropriate for this sample of weak scintillation. At the -1 dB fade level, the flat top portion of the curve commences to slope downwards at a fade duration of 0.2 sec, which represents the longest fade duration at this fade level.

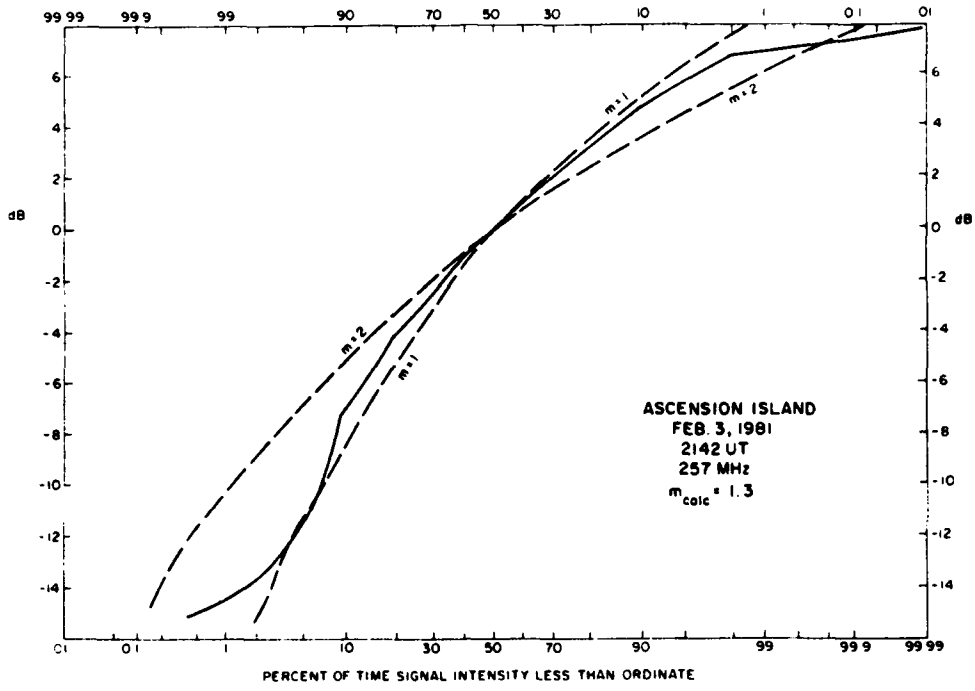

Figure 2c. The Cumulative Amplitude Distributions of Scintillations at 257 MHz Shown in Figure 1. Two theoretical Nakagami-m distributions with m = 1 and m = 2 are shown to contain the experimental distribution .

The maximum number of fades encountered at -1 dB level is 54. This number reduces with decrease in fade duration and attains a count of 27, that is, 50 percent of the maximum count at a fade duration of 0.08 sec. At the next lower fade level of -2 dB the maximum number of fades reduces to 22. The -4 dB fade level lies on the abscissa indicating that fadings do not reach this level. The right-hand panel shows the corresponding distribution for 1541 MHz scintillation which is much more intense and is, in fact, saturated at S_4 1.12. In this case, the fade levels are chosen at wider intervals. The distribution is interesting in the sense that the number of fades are drastically reduced at higher fade levels exceeding -16 dB. Thus, although the fade depth of strong 1541 MHz scintillation exceeds 20 dB, the number of fades at -16 dB level in one 1.5 min interval is only seven and the maximum fade duration does not exceed 0.1 sec.

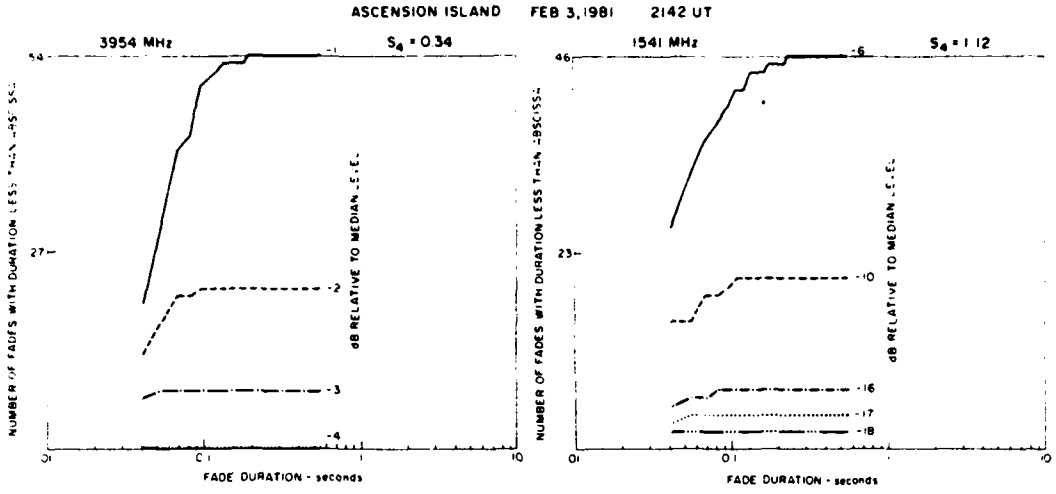

Figure 3. Distribution of the Fade Durations for the Period of Weak Scintillations at 3954 MHz and Strong Scintillations at 1541 MHz Illustrated in Figure 1

We shall next concentrate on the results of both intensity and phase measurements at Ascension Island performed with the computer-controlled receiver discussed in Section 2. These measurements were performed by the use of 244-MHz transmissions from Fleetsatcom. The intensity and phase scintillation data were analyzed over successive 150-sec periods. Since the 257 MHz intensity scintillation data acquired from the Marisat satellite have already been discussed in the previous paragraphs, we shall comment primarily on the phase scintillation data which are quite unique and are being reported here for the first time.

Figure 4 shows the 50th and 90th percentile of S_4 index of intensity scintillation (defined earlier) and rms phase deviation (σ_φ) over 150-sec periods detrended with a 0.01 Hz filter as a function of local time. The time interval corresponds to the post-sunset to post-midnight period (20-04L.T) when equatorial F-region irregularities are most intense and abundant. The period January-February 1981 corresponds to a period of high scintillation occurrence as previously mentioned. The number of data points in each 2-hourly block is indicated along the abscissa. It may be noted that in the early evening hours between 20-22LT, both the median and 90th percentile values of S_4 and σ_φ are highly elevated. The intensity scintillation data saturated at a level of approximately $S_4 = 0.8$ because of receiver constraints. With the Marisat satellite we have shown that both VHF and L-band intensity scintillations at this station become saturated with $S_4 \approx 1.0$ The saturation of intensity scintillation data at about 0.8 did not, however, affect phase measurements. It may be noted that the 90th percentile of rms phase deviation at

20 to 22-hour block is as large as 16 rads with 100-sec detrend. In a similar propagation geometry, the values of rms phase deviation may be scaled to shorter detrend intervals (T_d) by multiplying the given values by $T_d/100^{(p-1)/2}$, where p (~2.5) is the phase spectral index.[26] From Figure 4, it may also be noted that the 50th and 90th percentile values of these scintillation parameters decrease sharply with increasing local time owing to the decay of irregularity strength.

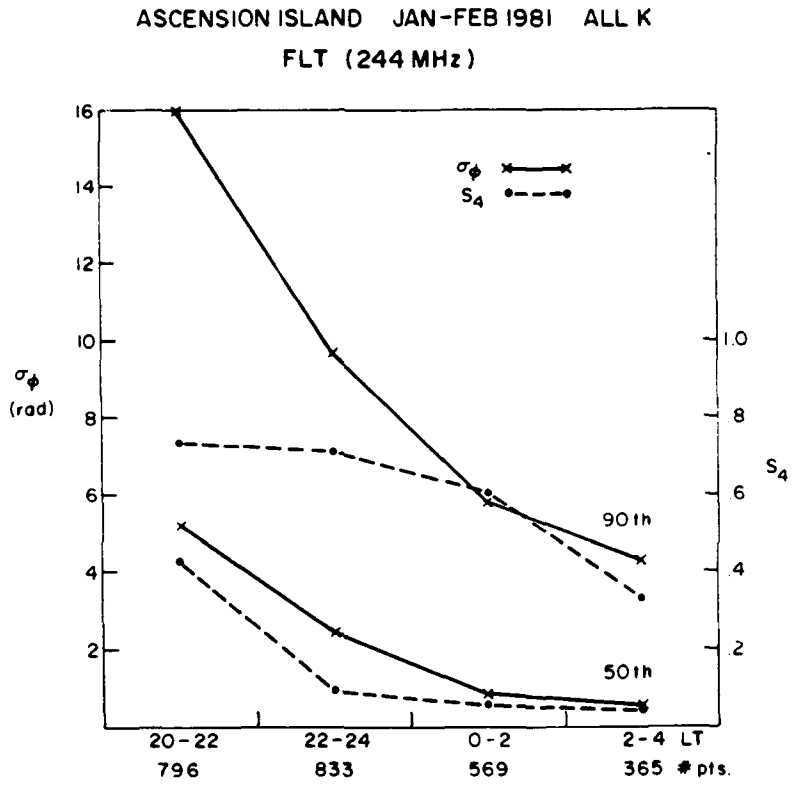

Figure 4. The Median (50th Percentile) and 90th Percentile Values of Phase and Intensity Scintillations at 244 MHz in Terms of Four 2-hr Blocks of Local Time (LT) During January-February 1981 at Ascension Island. Number of points in each bin is also indicated along the abscissa

26. Rino, C. L., and Owen, J. (1980) The time structure of transionospheric radio wave scintillation, Radio Sci., 15:479.

We shall now discuss the 244-MHz phase scintillation data that were acquired from the Fleetsat satellite at Ascension Island on 3 February 1981. Multi-frequency intensity scintillation data from the Marisat satellite for this day has already been presented earlier. Figure 5 shows a sequence of phase scintillation data over successive 88-sec intervals and their spectra obtained by the maximum entropy method[27] in the adjacent panels. The signal segments and their spectra are numbered on the left-hand side of each panel for ease of comparison. The rms phase deviation in radians for each 88-sec interval is indicated on the right-hand side of the data segments. The initial data segments with no activity are not shown and the panels start from the 34th data segment, which commences at 222430 UT. The first two data segments (34 and 35) show very little phase variations. The corresponding phase spectra show that the noise floor extends from the Nyquist frequency of 25 Hz to about 0.2 Hz. Phase power spectral densities (psd) are noticeable only at lower frequencies. A sudden onset of scintillations may be noted in the third panel. The corresponding spectra indicates an abrupt increase of psd at all frequencies up to 25 Hz. The numbers alongside the spectra indicate the magnitude of maximum instantaneous spectral slopes. The spectral slopes attain values ranging between -2 to -2.5 during the period of scintillations but remain much higher before the onset of scintillations as may be noted from the first two spectra. It is worthwhile to recall that the spectral slope of intensity scintillations at a similar frequency (cf. Figure 1) and a similar period of intense activity is very steep. This is caused by the refractive effects of large scale irregularities of electron density on the structure of intensity scintillations.[21,22] Until recently, one expected that the spectra of weak intensity scintillations and phase scintillations of any magnitude would reflect the slope of irregularity spectra in the ionosphere. In fact, the slope of -4.2 in the weak scintillation spectrum at 3954 MHz as shown in Figure 1 reflects very well the average one-dimensional irregularity spectral slope of -3.5 at small scales.[18] The spectral slopes of strong phase scintillations at 244 MHz, however, indicate shallow spectral slopes in the vicinity of -2.5. The apparent discrepancy has been resolved by Rino and Owen.[28] They simulated an ionospheric phase screen, allowed a radio wave to propagate through it, and computed numerically the phase structure and phase spectra at various distances from the screen. They showed that due to the diffractive effects of phase in a strong scattering medium, the phase structure develops large, near discontinuous, phase

27. Fougere, P.F. (1985) On the accuracy of spectrum analysis of red noise processes using maximum entropy and periodogram methods: simulation studies and application to geophysical data, J. Geophys. Res., 90:4355-4366.

28. Rino, C.L., and Owen, J. (1984) Numerical simulations of intensity scintillation using the power law phase screen model, Radio Sci., 19:891.

changes (termed 'cycle slips') and yields phase spectra with slopes approaching -2.

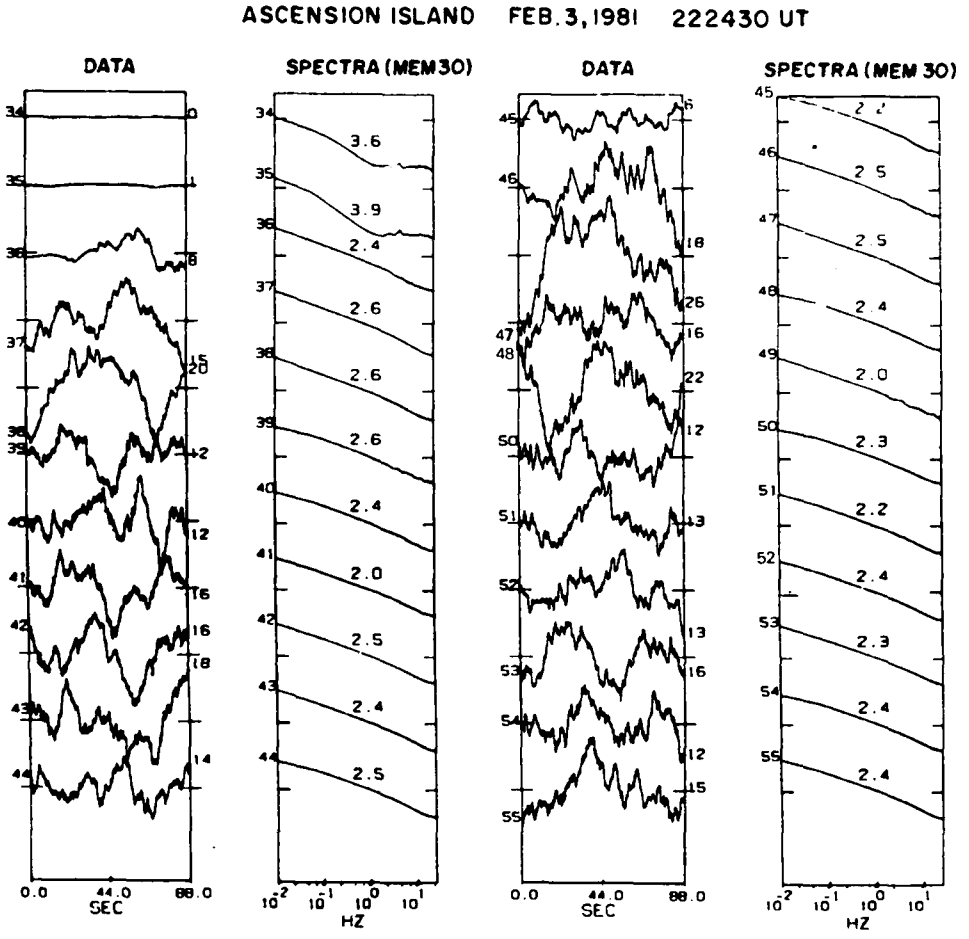

Figure 5. Phase Scintillation Data Segments at 244 MHz Over 88-sec Intervals and Their Spectra in Alternate Panels. The data were acquired at Ascension Island on 3 February 1981 by the use of transmissions from Fleetsatcom satellite. The intervals between the tic marks on the data panel represent 50 rad and on the spectral panel psd of 80 dB. The left-hand side of the panels indicate the numerical sequence of the data and their spectra. The right-hand side of the data panels indicates rms phase deviations. The numbers on the spectra indicate maximum instantaneous power law index of the roll-off portions of the spectra

Figure 6 shows a scatter plot of phase spectral slope vs phase spectral strength in decibels that is defined as the phase psd at 1 Hz when the S_4 index exceeds 0.6, that is, for strong scintillations. The data were acquired at Ascension Island during January-February 1981. At low values of phase spectral strengths or high decibel numbers, phase spectral slopes show a wide scatter between -2 and -2.9 in Figure 6, but at high values of phase psd the slopes approach a value of -2. This provides observational support to the 'cycle slip' argument presented in the previous paragraph.

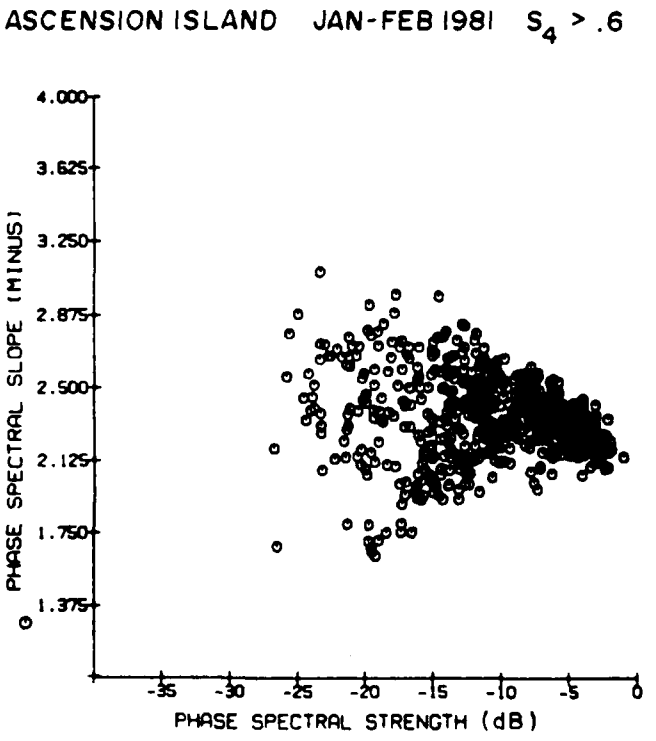

Figure 6. A Scatter Plot of the Phase Spectral Slope Against Phase Spectral Strength (dB) at Ascension Island at 244 MHz. The slope approaches a value of -2 at high phase spectral strengths

In Figure 7, we show an interesting plot of intensity decorrelation time at 244 MHz on a logarithmic scale against phase spectral strength (decibels) for strong scintillations ($S_4 > 0.6$). It may be noted that with increased phase spectral strengths in this regime, the intensity scintillation systematically develop finer structures on the ground so that the decorrelation time decreases from about 1 sec to 0.05 sec.

By using the method outlined in Reference 26, it is possible to derive the average spectral slope from the slope of the best fit straight line to the scatter plot of Figure 7. The scatter diagram indicates a spectral slope of -2.4. This is in very good agreement with the phase spectral slopes of the data segments illustrated in Figure 5.

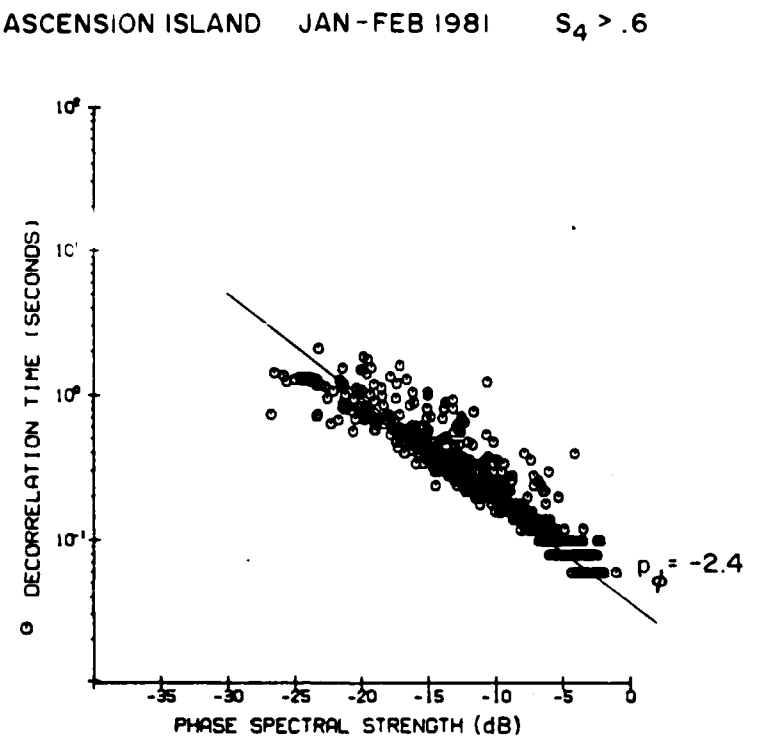

Figure 7. A Scatter Plot of Intensity Decorrelation Time Against the Phase Spectral Strength of 244 MHz Scintillations Recorded at Ascension Island. The theoretical dependence of the two parameters in the strong scatter regime for a phase spectral index $p_\phi = -2.4$ is indicated by the straight line

The results shown in Figures 6 and 7 imply that in the disturbed equatorial ionosphere, the structures of intensity and phase scintillations are controlled by the strength of scattering. The decorrelation time is a function of the spatial structure of intensity variation on the ground as well as the ionospheric drift which controls the motion of the spatial structure past a receiving antenna. The fact that the decorrelation time is so well ordered, in terms of the phase spectral strength, indicates that the drift velocity does not vary much between the post-sunset and the

midnight period, and it is the strength of the irregularities that control primarily the fading pattern of scintillations. This is, however, not true at high latitudes where the phase spectral strength or the integrated strength of irregularities is not as intense as in the equatorial region, but the drift velocity can vary by an order of magnitude within a short interval of time. At high latitudes, therefore, the fading pattern is primarily controlled by the irregularity drift.

From Figure 5 it was evident that in intense equatorial phase scintillation events, considerable power resides in the regime of high fluctuation frequencies. This is equivalent to stating that the probability of having a high rate of change of phase is considerable. The phase rate, on the other hand, is a measure of the Doppler spread the signal undergoes in traversing the irregularities of the ionosphere. In Figure 8, the probability distribution of the phase rate in phase scintillations has been computed over 0.1-sec intervals during a 30-min period of intense scintillations at Ascension Island. Since the Nyquist frequency is 25 Hz, the phase rate could have been computed over a much shorter time interval. However, at sampling intervals the noise becomes comparable to the signal and the derived phase rates would have been contaminated by the phase rate of noise signals. In Figure 8a, the occurrence of phase rate between $\pm 500°$ sec^{-1} has been plotted. It is found that nearly 20 percent of the total population (10^5 points) contains phase rates in excess of $\pm 500°$ sec^{-1}. The distribution of population with extreme phase rates has been plotted in Figure 8b over a wider range extending from ± 500 to $\pm 2300°$ sec^{-1}. It may be noted that phase rates as high as $2000°$ sec^{-1} or $2°$ $msec^{-1}$ occur in 0.1 percent of the population with extreme phase rates which, in turn, represents 20 percent of the total number of observations during approximately a half-hour period. Such extreme phase rates have considerable deleterious effects on radar systems. Since the phase scintillation magnitude varies inversely as frequency,[29] the above phase rate may be scaled from the 244-MHz observations to 2.4 GHz as $0.2°$ $msec^{-1}$.

---

29. Fremouw, E. J., Leadabrand, R. L., Livingston, R. C., Cousins, M. D., Rino, C. L., Fair, B. C., and Long, R. A. (1978) Early results from the DNA Wideband satellite experiment—complex-signal scintillation, Radio Sci., 13:167.

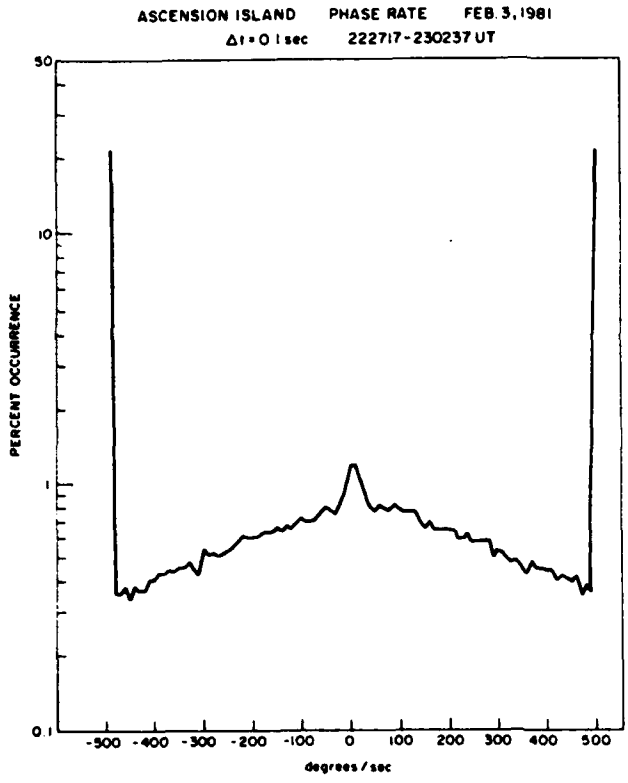

Figure 8a. The Distribution of Phase Rate of 244 MHz Scintillation at Ascension Island. The high values at the two ends indicate percent occurrence of values > 500° sec^{-1}

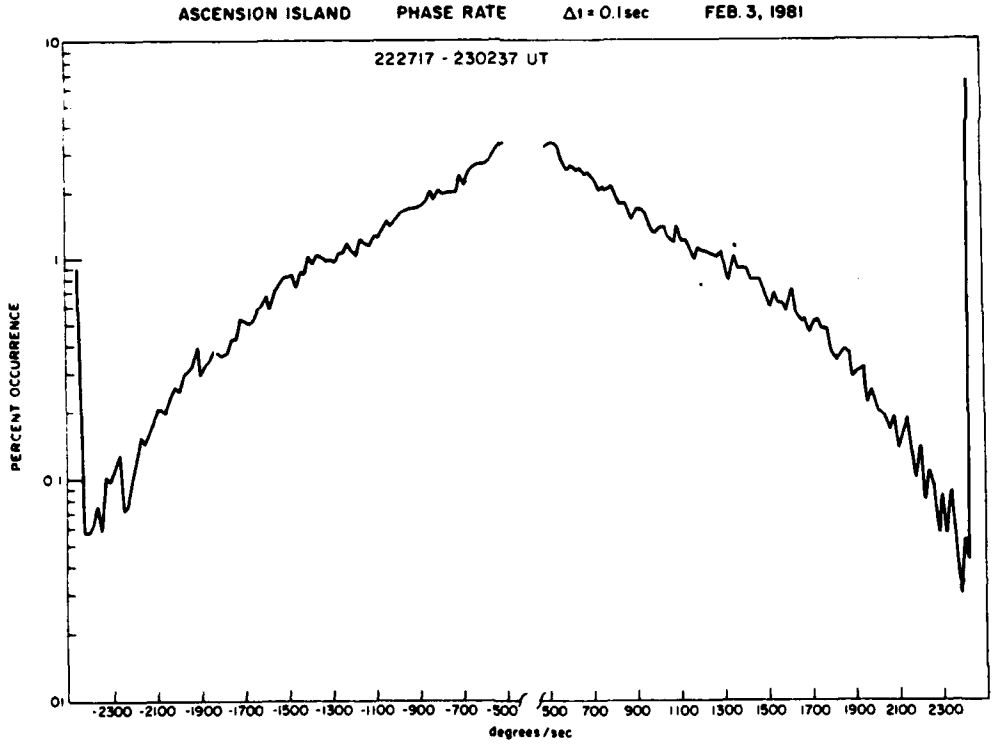

Figure 8b. The Distribution of the Population With Extreme Phase Rates Which Correspond to the Two Ends of the Diagram in Figure 8a

3.2 Thule, Greenland

At Thule, a polar cap station, the phase and intensity scintillation data were acquired by receiving 250 MHz transmissions from the near-stationary Air Force satellites at high elevation angles. The ionospheric intersection of the ray path covered a corrected geomagnetic latitude range of 85° - 89° N. Since scintillations are better ordered in terms of corrected geomagnetic latitude (CGLAT) and magnetic local time (MLT) at high latitudes, we shall use this system of coordinates as described in Reference 30. The phase and intensity measurements were made with the computer controlled phase lock receiver during specified intervals as mentioned in Section 2.

The morphology of intensity scintillations[31] and that of both phase and intensity scintillations[5] from Thule have been discussed earlier. In this report, we shall present phase and intensity scintillation data during January-February 1982 not previously published, and use it to contrast its behavior against the Ascension Island observations. We have also extended the intensity scintillation morphology further through the years of low sunspot number to illustrate the control of solar activity on polar cap scintillations.

Figure 9 shows the variation of 250 MHz intensity scintillation index (S_4) and rms phase deviation (σ_φ) over 82-sec intervals with magnetic local time as observed at Thule during January-February 1982. It may be noted that at Thule the scintillation activity during years of high sunspot numbers persists at all hours, the median value of phase remaining between 3 and 5 rads over the entire diurnal period. This behavior is in sharp contrast to that at Ascension Island, an equatorial station, where strong scintillations are, in general, confined between the post-sunset to midnight hours. In view of this, the scintillation statistics in Figure 4 were derived between 20-04 LT. At auroral locations, such as Goose Bay, scintillations on magnetically quiet days are again confined to nighttime periods as discussed in Reference 5. Thus, an absence of diurnal variation of scintillations during periods of high solar activity is a feature confined only to the polar cap. The level of 250-MHz scintillations is also high, the 90th percentiles of rms phase attaining values as high as 12 rads and intensity scintillations remaining near saturation with $S_4 \sim 0.9$.

---

30. Whalen, J.A. (1970) Auroral Oval Plotter and Nomograph for Determining Corrected Geomagnetic Local Time, Latitude and Longitude for High Latitudes in the Northern Hemisphere, AFCRL-TR-70-0422, AD 713170, Air Force Cambridge Research Laboratory, Hanscom AFB, Massachusetts.

31. Aarons, J., Mullen, J.P., Whitney, H.E., Johnson, A., and Weber, E. (1981) VHF scintillation activity over polar latitudes, Geophys. Res., Lett., 8:277.

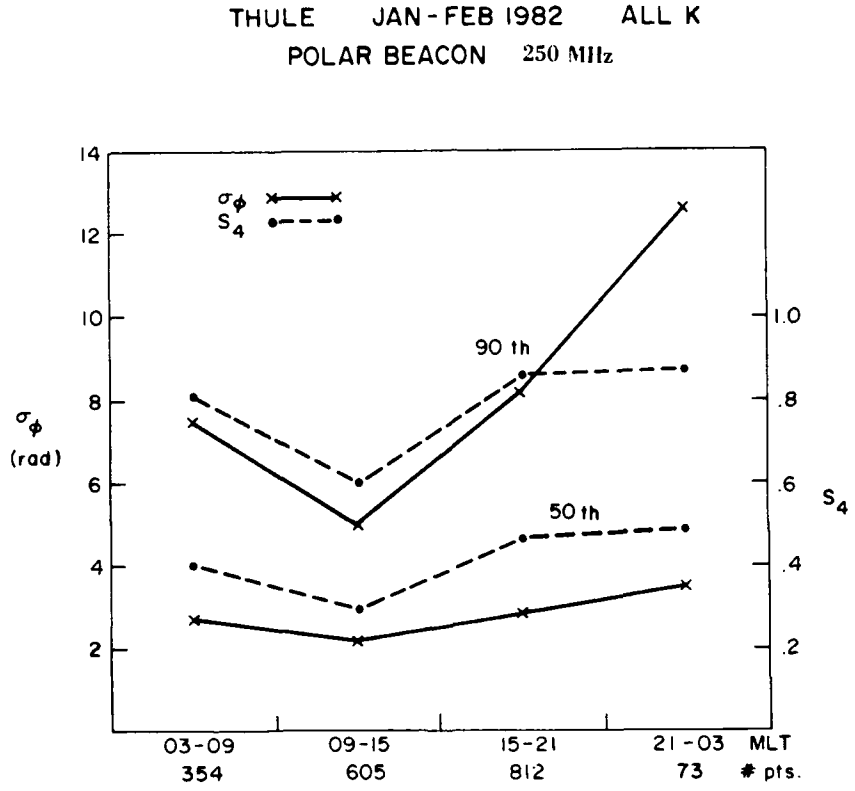

Figure 9. The Median (50th Percentile) and the 90th Percentile Values of Phase and Intensity Scintillation at 250 MHz in Terms of Four 6-hr MLT Blocks Observed at Thule

The long term statistics of 250-MHz intensity scintillations derived with total power receiving systems are shown in Figure 10. The figure shows the variation of scintillation occurrence at various fade depths for 1979 to 1984. The highest fade level of ≥ 20 dB represents a peak-to-peak fluctuation level of ≥ 28 dB. The scintillations minimize during the summer months so that the annual variation becomes most conspicuous. During the sunlit period, the high conductivity at E-region heights (~100 km) is not favorable for the maintenance of irregularities in the overlying F-region of the ionosphere.[32] In other periods, particularly during the autumnal equinox, fade depths as large as 20 dB with 20 percent occurrence could be obtained up to 1982. The scintillation activity did not vary much during the period 1979 to 1982 when sunspot numbers varied between 200 and 100. With further reduction of sunspot numbers, scintillations showed abrupt decline during 1983 and 1984. Thus, there seems to be a lower threshold of solar activity below which irregularities of sufficient integrated strength are not encountered.

32. Vickrey, J.F., and Kelley, M.C. (1982) The effects of a conducting E layer on classical F-region cross-field plasma diffusion, J. Geophys. Res., 87:4461.

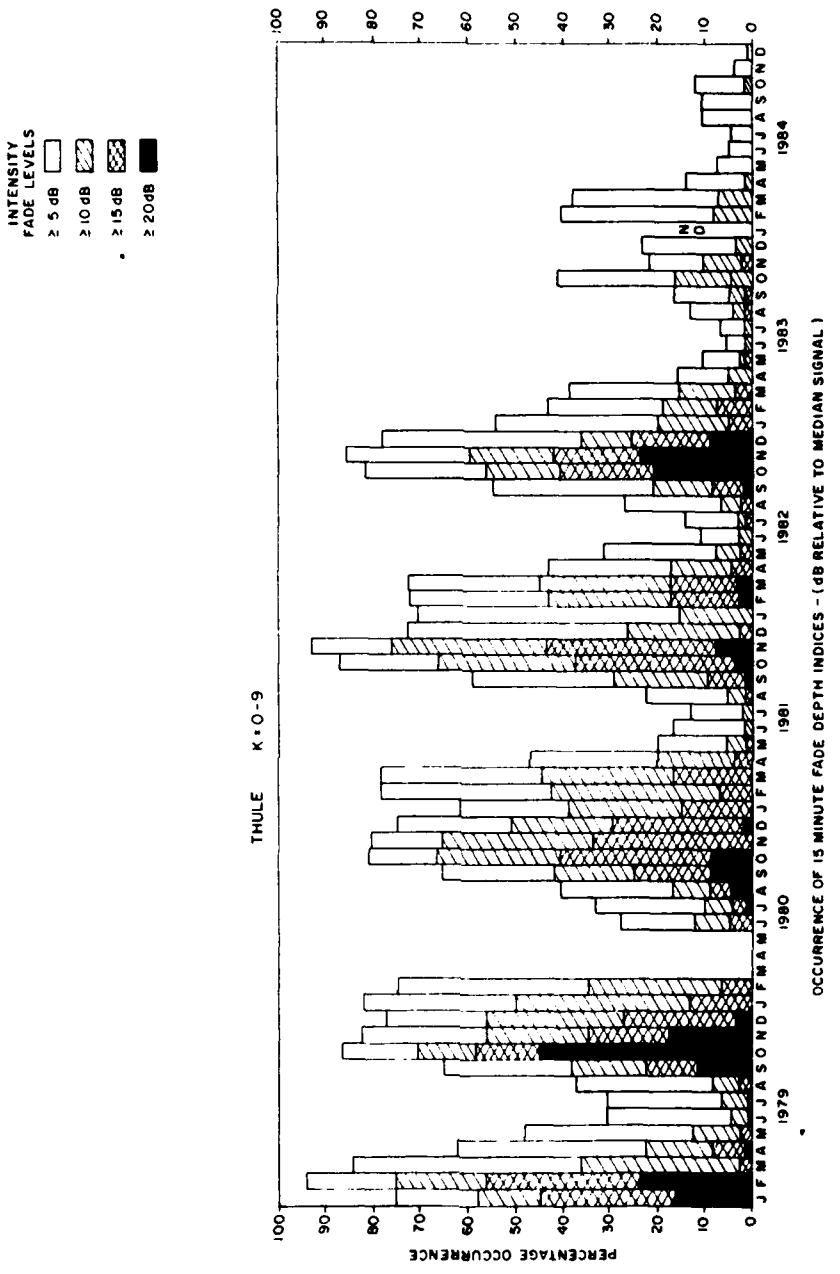

Figure 10. Thule Intensity Scintillation Statistics at 250 MHz During 1979 to 1984

Figure 11 shows the occurrence contours of fade levels that exceed 10 dB on both a monthly and diurnal basis. As pointed out in the previous paragraphs, the annual variation of scintillations is the more prominent feature and the diurnal variation is virtually absent at Thule. However, there emerges a diurnal pattern in the October-November period that becomes most conspicuous during the low sunspot years of 1983 and 1984. The maximum activity during these months seems to be confined to the afternoon period around 15 MLT.

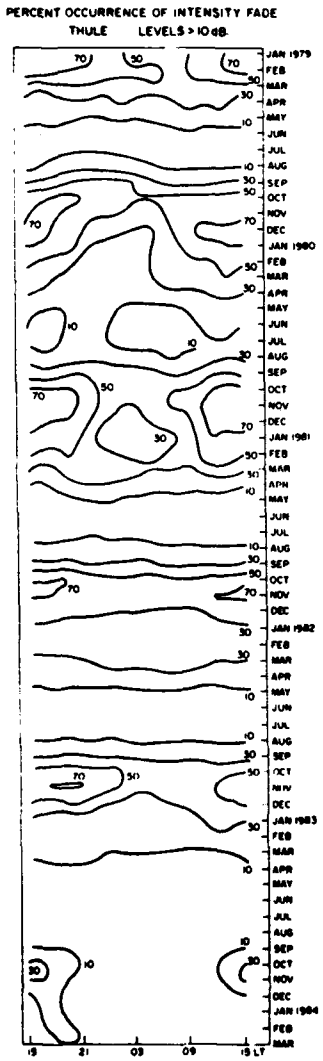

Figure 11. Intensity Scintillations at Thule at 250 MHz on a Seasonal and Local Time Basis. The contour levels represent percent occurrence

The strong scintillation events with S_4 exceeding 0.6 that could be recorded by the phase-lock receiving system were sorted. The intensity decorrelation time and phase spectral strengths were determined and their mutual dependence is plotted in Figure 12. The best fit straight line through the scatter plots corresponded to the theoretical dependence[26] expected for the case of strong scattering with phase spectral slope of -2.2. It signifies that during strong scintillations at Thule, the intensity scintillation structure is largely governed by the phase spectral strength. Increased scatter around the best-fit line signifies that the drift speed may vary by a factor of 3-4. On the other hand, the scatter in Figure 7 is much less, indicating that the variation of drift speed is small in the equatorial region. At the auroral station of Goose Bay, a similar plot (not shown here) indicates considerable scatter as well due to the high variability of drift speeds.

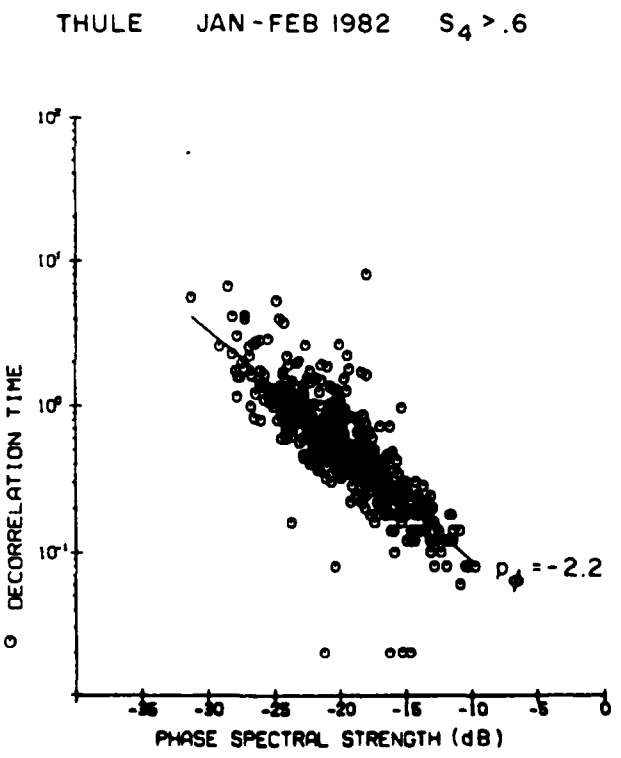

Figure 12. A Scatter Plot of the Intensity Decorrelation Time Against Phase Spectral Strength Observed at Thule at 250 MHz. The theoretical dependence of the two parameters for a phase spectral index of -2.2 is indicated by the straight line

3.3 Goose Bay, Labrador

We shall not discuss in great detail the features of scintillations at Goose Bay, an auroral station, but refer to Reference 5 which compared the characteristics of polar cap and auroral scintillations. In short, the auroral station shows a well-ordered diurnal variation of scintillations with a nighttime maximum and daytime minimum, whereas we have shown the absence of such ordering in the polar cap region, such as Thule. The auroral scintillation magnitudes are, on the average, similar to that in the polar cap although, on occasions, more active conditions prevail in the polar cap. The polar cap scintillation pattern exhibits the presence of discrete structures, whereas in the auroral oval intense scintillation events continue for hours without showing much variation in magnitude. The major feature of an auroral station is the extreme variability of drift speed. It is not uncommon to observe a change in speed from 100 m sec^{-1} to 1000 m sec^{-1} within a 30-min period. This variability in speed affects greatly the temporal structure parameters of scintillations such as the decorrelation time or the rate of change of phase and intensity. Figure 13 shows the rate of change of intensity encountered on two successive nights, 7 March and 8 March 1982. The scheme of the plot is similar to the phase rate plot in Figure 8a for Ascension Island, except for the longer data interval (0.5 sec) used to compute the rates at the auroral location. Shorter time intervals could not be used here because of possible noise contamination. At the equatorial station, intervals as short as 0.1 sec could be used to compute phase rates as high levels of ionospheric turbulence developed high frequency structures much above the noise floor. Figure 13 shows that at Goose Bay, on 7 March 1982, the intensity rate of 3 dB sec^{-1} occurs in 0.1 percent of the total population whereas it increases to about 7 dB sec^{-1} at the same 0.1 percent level on 8 March 1982. Intensity spectral studies revealed that the irregularity drift speed was 65 m sec^{-1} on 7 March 1982 and increased to 390 m sec^{-1} on 8 March 1982.[5] The six-fold increase in drift speed is reflected in increased intensity rates. Figure 14 shows the phase rate plots for the two days. It may be noted that at 0.1 percent level, the phase rate may attain values as high as 250° sec^{-1} at an auroral location when drift speed is high. If the change can be linearly extrapolated, the above value translates to 0.25 m sec^{-1}. This is an order of magnitude smaller than the phase encountered at Ascension Island and illustrated in Figure 8b.

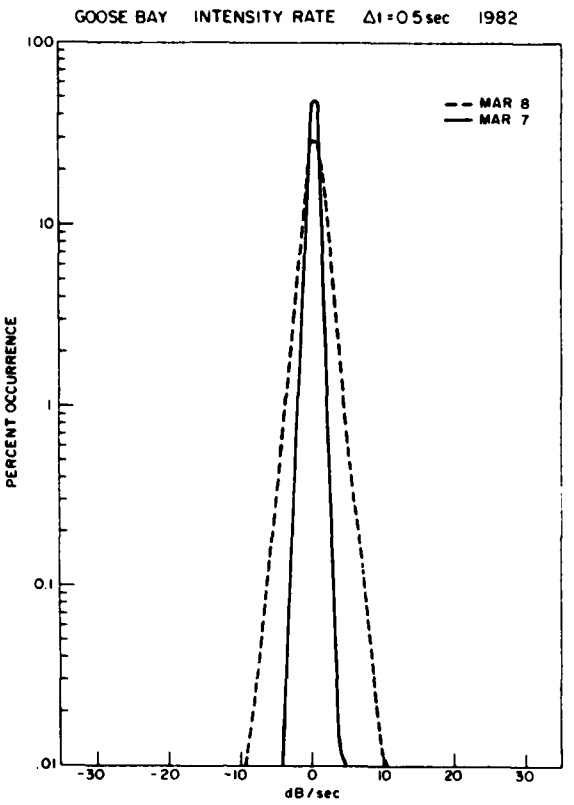

Figure 13. The Distribution of Intensity Rate of Scintillations at 250 MHz at Goose Bay on Two Successive Nights With Different Ionospheric Drifts. The drift was lower on 7 March by a factor of six as compared to 8 March

4. CONCLUSIONS

The results on the structure of multi-frequency amplitude scintillations covering the VHF (257 MHz) to C-band (3954 MHz) frequencies at the crest of the equatorial anomaly and the structure of 250-MHz phase and amplitude scintillations in the equatorial anomaly, auroral and polar cap regions can be summarized as follows.

At Ascension Island, located at the crest of the equatorial anomaly, the most disturbed irregularity environment on a global basis was encountered during the last sunspot maximum period. At this location, the disturbance level was so intense

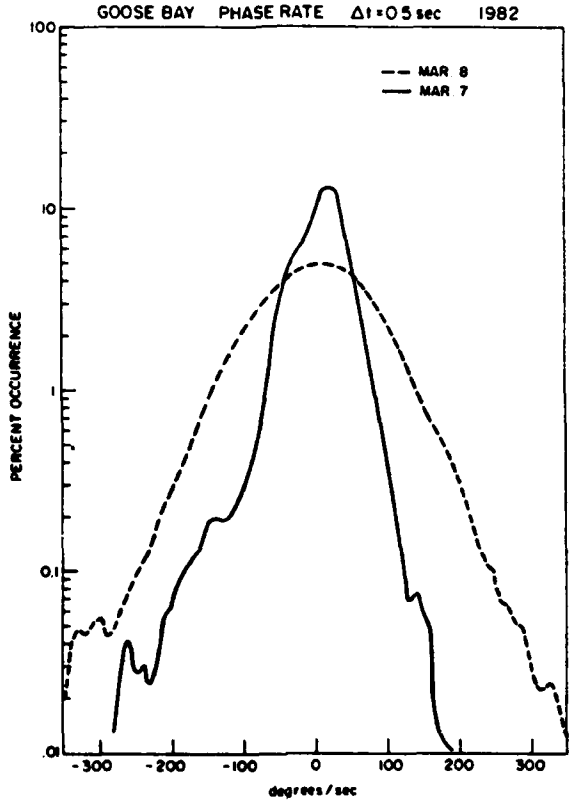

Figure 14. The Distribution of 250 MHz Rate of Phase Scintillations at Goose Bay on Two Successive Nights to Indicate the Change of Distribution With Variation of Ionospheric Motion. On 7 March the drift velocity was lower than on 8 March

that not only the VHF (250 MHz) but also the L-band (1541 MHz) transmissions from geostationary satellites exhibited saturated intensity scintillations which covered the 30 dB dynamic range of receivers that were used to record the satellite transmissions. Even the transmissions at 4 GHz registered fluctuations as large as 6 dB. The median and the 90th percentile values of rms phase deviation at 244 MHz with 100-sec detrend are 6 and 16 rad, respectively, during the early evening hours. The phase spectral strengths (phase psd at 1 Hz) which indicate the strength of turbulence are found to attain values as high as -2 dB. This is at least 10 dB above the most intense levels that are obtained at the polar cap or auroral stations. The extreme levels of turbulence at Ascension Island induce strong scattering of VHF and L-band signals and thereby dictate the structures of amplitude and phase

scintillations at both frequencies. The amplitude scintillation spectra at VHF and L-band under such situations show uniform psd up to fluctuation frequencies as high as a few Hz and give rise to steep power law spectral indices of -5 to -7. The intensity decorrelation times are consequently reduced to values as low as 0.06 sec at VHF. The phase spectral slopes at 244 MHz approach a value of -2.5 which is much shallower than is expected from either the in situ irregularity spectra or weak amplitude scintillation spectra at 4 GHz. This probably arises from sharp discontinuous phase changes or 'cycle slips'[28] that develop due to phase diffraction effects under strong scatter conditions. In view of these discontinuous phase changes, extreme phase rates of 2-3° $msec^{-1}$ were observed. This is rather significant for UHF radar applications.

In the polar cap (Thule), the median and 90th percentile values of rms phase deviation at 250 MHz for 82-sec detrend are observed to be 3 and 12 rad respectively. The corresponding values for the S_4 index of scintillations are 0.5 and 0.8. These values are in reasonable agreement with those published in Reference 5 for another period of observations. The point of interest is the absence of any diurnal variation of polar cap scintillations, its annual variation with a pronounced minimum during local summer, and rather abrupt decrease of scintillations when the solar activity decreases below a threshold level. The irregularity spectral strengths in the polar cap or auroral stations are shown to be not as intense as in the equatorial region. At high latitudes the phase spectral indices of about -2.2 cannot be attributed to strong scattering effects, but is probably a result of shallow irregularity spectral indices in the ionosphere. At auroral locations, the variability of ionospheric motion greatly controls the temporal structure of scintillations. The phase rates are typically of the order of 0.2-0.3° $msec^{-1}$, but may show considerable changes due to the variability of ionospheric motion.

References

1. Aarons, J. (1982) Global morphology of ionospheric scintillation, Proc. IEEE, 70:360-278.

2. Livingston, R.C. (1980) Comparison of multifrequency equatorial scintillation: American and Pacific sectors, Radio Sci., 15:801.

3. Rino, C.L., and Matthews, S.J. (1980) On the morphology of auroral zone radio wave scintillation, J. Geophys. Res., 85:4139.

4. Basu, Su., Basu, S., Livingston, R.C., Whitney, H.E., and MacKenzie, E. (1981) Comparison of Ionospheric Scintillation Statistics From the North Atlantic and Alaskan Sectors of the Auroral Oval Using the WIDEBAND Satellite, Rpt. AFGL-TR-81-0266, AD A111871, Air Force Geophysics Laboratory, Hanscom AFB, Massachusetts.

5. Basu, Su., Basu, S., MacKenzie, E., and Whitney, H.E. (1985) Morphology of phase and intensity scintillations in the auroral oval and polar cap, Radio Sci., 20:347-356.

6. Rino, C.L., Livingston, R.C., Tsunoda, R.T., Robinson, R.M., Vickrey, J.F., Senior, C., Cousins, M.D., Owen, J., and Klobuchar, J.A. (1983) Recent studies of the structure and morphology of auroral zone F-region irregularities, Radio Sci., 18:1167-1180.

7. Basu, Su., and Basu, S. (1985) Equatorial scintillations: advances since ISEA-6, J. Atmos. Terr. Phys., 47:753-768.

8. Basu, Su., Basu, S., Senior, C., Weimer, D., Nielsen, E., and Fougere, P.F. (1986) Velocity shears and sub-km scale irregularities in the nighttime auroral F-region, Geophys. Res. Lett., 13:101.

9. Fremouw, E.J., and Secan, J.A. (1984) Modeling and scientific application of scintillation results, Radio Sci., 19:687-694.

10. Basu, Su., Basu, S., Livingston, R.C., MacKenzie, E., and Whitney, H.E. (1982) Phase and amplitude scintillation statistics at 244 MHz From Goose Bay Using a Geostationary Satellite, Rpt. AFGL-TR-82-0222, AD A124291, Air Force Geophysics Laboratory, Hanscom AFB, Massachusetts.

References

11. Basu, Su., MacKenzie, E., Basu, S., Carlson, H.C., Hardy, D.A., Rich, F.J., and Livingston, R.C. (1983) Coordinated measurements of low-energy electron precipitation and scintillations/TEC in the auroral oval, Radio Sci., 18:1151.

12. Whitney, H.E., and Basu, S. (1977) The effect of ionospheric scintillation on VHF/UHF satellite communications, Radio Sci., 12:123.

13. Aarons, J., Whitney, H.E., MacKenzie, E., and Basu, S. (1981) Microwave equatorial scintillation intensity during solar maximum, Radio Sci., 16:939-945.

14. Mullen, J.P., MacKenzie, E., Basu, S., and Whitney, H.E. (1985) VHF/GHz scintillation observed at Ascension Island from 1980 through 1982, Radio Sci., 20:357-365.

15. Briggs, B.H., and Parkin, I.A. (1963) On the variation of radio star and satellite scintillation with zenith angle, J. Atmos. Terr. Phys., 25:339-365.

16. Rufenach, C.L. (1974) Wavelength dependence of radio scintillation: Ionosphere and interplanetary irregularities, J. Geophys. Res., 79:1562-1566.

17. Whitney, H.E. (1974) Notes on the Relationship of Scintillation Index to Probability Distributions and Their Uses for System Design, Rpt. AFCRL-TR-74-0004, AD 778092, Air Force Cambridge Research Laboratory, Hanscom AFB, Massachusetts.

18. Basu, Su., Basu, S., McClure, J.P., Hanson, W.B., and Whitney, H.E. (1983) High-resolution topside in-situ data of electron densities and VHF/GHz scintillations in the equatorial region, J. Geophys. Res., 88:403.

19. Franke, S.J., and Liu, C.H. (1983) Observations and modeling of multifrequency VHF and GHz scintillations in the equatorial region, J. Geophys. Res., 88:7075.

20. Basu, S., and Whitney, H.E. (1983) The temporal structure of intensity scintillations near the magnetic equator, Radio Sci., 18:263.

21. Rino, C.L. (1980) Numerical computations for a one-dimensional power law phase screen, Radio Sci., 14:41.

22. Booker, H.G., and MajidiAhi, G. (1981) Theory of refractive scattering in scintillation phenomena, J. Atmos. Terr. Phys., 43:1199.

23. Umeki, R., Lui, C.H., and Yeh, K.C. (1977) Multifrequency studies of ionospheric scintillations, Radio Sci., 12:311.

24. Nakagami, M. (1980) The m-distribution—a general formula of intensity distribution of rapid fading, Statistical Methods of Radio Wave Propagation, W.C. Hoffman, Eds., Symposium Publications Div., Pergamon Press, New York.

25. Whitney, H.E., Aarons, J., Allen, R.S., and Seeman, D.R. (1972) Estimation of the cumulative amplitude probability distribution function of ionospheric scintillations, Radio Sci., 7:1095-1104.

26. Rino, C.L., and Owen, J. (1980) The time structure of transionospheric radio wave scintillation, Radio Sci., 15:479.

27. Fougere, P.F. (1985) On the accuracy of spectrum analysis of red noise processes using maximum entropy and periodogram methods: simulation studies and application to geophysical data, J. Geophys. Res., 90:4355-4366.

28. Rino, C. L., and Owen, J. (1984) Numerical simulations of intensity scintillation using the power law phase screen model, Radio Sci., 19:891.

29. Fremouw, E. J., Leadabrand, R. L., Livingston, R. C., Cousins, M. D., Rino, C. L., Fair, B. C., and Long, R. A. (1978) Early results from the DNA Wideband satellite experiment—complex-signal scintillation, Radio Sci., 13:167

30. Whalen, J. A. (1970) Auroral Oval Plotter and Nomograph for Determining Corrected Geomagnetic Local Time, Latitude and Longitude for High Latitudes in the Northern Hemisphere, AFCRL-TR-70-0422, AD 713170, Air Force Cambridge Research Laboratory, Hanscom AFB, Massachusetts.

31. Aarons, J., Mullen, J. P., Whitney, H. E., Johnson, A., and Weber, E. (1981) VHF scintillation activity over polar latitudes, Geophys. Res. Lett., 8:277.

32. Vickrey, J. F., and Kelley, M. C. (1982) The effects of a conducting E layer on classical F-region cross-field plasma diffusion, J. Geophys. Res., 87:4461.

END

10-86

DTIC